ORIGINAL ARTICLE

Diagnostic Accuracy of MRI and CT Scan Features in Differentiation of Pediatric Ependymoma from Medulloblastoma

Sam Mirfendereski, MD [1] ; Neda Mansouri, MD [1]

[1] Department of Radiology, Isfahan University of Medical Sciences, Isfahan, Iran

Keywords:

Ependymoma
Medulloblatoma
Apparent Diffusion Coefficient
MRI
CT

Received:
07- May -2023
Accepted:
08-Jul-2024
Published:
07-Jan-2025

ABSTRACT

Objectives

The study aims to compare the diagnostic accuracy of MRI and CT scan features in differentiating medulloblastoma from ependymoma, two similar pediatric brain tumors.

Materials & Methods

This retrospective cross-sectional study was conducted on all pediatric patients with posterior fossa tumors admitted to teaching hospitals affiliated with Isfahan University of Medical Sciences from 2017 to 2022. Forty-three patients with posterior fossa tumors were identified, and seven patients were excluded due to diagnoses other than medulloblastoma or ependymoma. Tumor morphology on MRI, tumor density on CT scan, and apparent diffusion coefficient (ADC) values were assessed to differentiate medulloblastoma from ependymoma.

Results

Histopathologic diagnosis was medulloblastoma in 21 patients (60%) and ependymoma in 14 patients (40%). Mean ADC values in medulloblastoma and ependymoma cases were 0.67±0.19 (range= 0.50-1.25) and 1.22±0.29 (range=0.67-1.72), showing a significant statistical difference between the two groups (p-value=0.000). The ADC cut-off point of 0.9825 was associated with 90% sensitivity and 92.9% specificity for differentiation of ependymoma from medulloblastoma.

Conclusion

While tumor morphology on MRI and other studied parameters are unreliable for differentiating medulloblastoma and ependymoma, ADC values may provide a potential diagnostic tool. Further studies are needed to confirm the utility of DWI and other advanced MRI techniques in differentiating these tumors.

How to cite this article: Mirfendereski S, Mansouri N. Diagnostic Accuracy of MRI and CT Scan Features in Differentiation of Pediatric Ependymoma from Medulloblastoma. Iran J Child Neurol. 2025; 19(1): 55-63. https://doi.org/10.22037/ijcn.v19i1.42100

*Corresponding Author: Mansouri N, MD. Department of Radiology, Isfahan University of Medical Sciences, Isfahan, Iran. Email: mtns94@gmail.com

Introduction

Brain tumors are the most prevalent solid neoplasms in children (1). Infratentorial tumors constitute 45 to 60 percent of pediatric brain tumors (2). The most common posterior fossa tumors are pilocytic astrocytoma (PA), medulloblastoma, ependymoma, and brainstem glioma (3). Medulloblastoma is the most common malignant brain tumor in children, accounting for approximately 20% of all childhood brain tumors (4, 5). It typically occurs in children between three and eight years old, with a slight male predominance (5). On the other hand, ependymoma is the third most common brain tumor in children, accounting for approximately 10% of all pediatric brain tumors. It has a bimodal age distribution, with a peak incidence in children under three years of age and another peak in children between six and nine years of age. Ependymoma is slightly more common in males than in females (6). Medulloblastoma and ependymoma are similar in several aspects. Symptoms and signs of these two tumors are generally alike, including headache, vomiting, disturbances in balance, papilledema, double vision, and irritability (7). Furthermore, Medulloblastoma and ependymoma typically develop from the fourth ventricle and nearby regions (8). In addition, they show similar features on MR images, including heterogeneous enhancement patterns due to calcification, necrosis, and hemorrhage (3, 7).

Accurate differentiation between these two tumor types is essential for appropriate treatment planning and improved patient outcomes. Although histopathological examination remains the gold standard for diagnosis, imaging modalities play a crucial role in the preoperative evaluation and differential diagnosis of these tumors. The clinical and imaging similarities of these tumors have led to diagnostic dilemmas in managing medulloblastoma and ependymoma in the pediatric population. Thus, efforts have been undertaken to describe differences between medulloblastoma and ependymoma in imaging studies. Reportedly, ependymomas are brighter on T2 sequences and more heterogeneous on MR images. Ependymomas usually lie in the base of the fourth ventricles and may extend through foramina. Moreover, evidence of obstructive hydrocephaly may be detected in ependymoma cases (9, 10). Despite these struggles to provide clues for differentiating these tumors, major overlapping features exist between ependymoma and medulloblastoma tumors. Studies have been conducted on morphologic characteristics, mass densities, and apparent diffusion coefficient (ADC) values to facilitate diagnosis and differentiate between these two entities (11). Most studies have been conducted on MRI, while few studies have investigated the efficacy of CT scan features in discriminating between medulloblastoma and ependymoma.

Despite the potential advantages of each imaging modality, there is still a lack of consensus on the most effective modality for differentiating medulloblastoma from ependymoma. This article aims to compare the diagnostic accuracy of MRI and CT scan features for this purpose.

Materials & Methods

This retrospective cross-sectional study was conducted in 2023 on all pediatric patients with posterior fossa tumors admitted to Alzahra, Imam-Hossein, and Kashani hospitals of Isfahan, Iran, from 2017 to 2022. Inclusion criteria were age under 15 years, presence of posterior fossa tumor, tumor diagnosis by neuroimaging and clinical confirmation of pediatric neurologist/

neurosurgeon, candidacy of tumor resection or tissue sampling, and parents' informed consent to participate in the study. Exclusion criteria included diagnoses other than medulloblastoma and ependymoma, unavailability of appropriate and high-quality images, and unwillingness to participate in the study. The Research Committee of Isfahan University of Medical Sciences approved the study. Then, demographic data of eligible patients meeting the inclusion criteria of the study were retrieved. Then, CT scan images were obtained from the digital archives of the hospitals. CT scans were reviewed by the expert radiologist, who was blinded to the histopathologic diagnosis of the patients. Tumor density in comparison to the adjacent brain tissue was determined. MR images were also re-evaluated by the expert radiologist, who was blinded to the definite diagnosis of the patient. A 1.5 Tesla GE MRI scanner performed all MRIs. The MRI protocol featured axial T1-weighted images, as well as axial and sagittal T2-weighted images, complemented by axial FLAIR and DWI images. After contrast injection, T1W images in coronal, axial, and sagittal views were acquired (planes (TR/TE= 4400/110 ms, NEX= 1220 mm FOV, 5-mm slice thickness, 1 mm interslice gap). Tumor morphology (presence of cystic component, heterogeneity pattern, hemorrhage), necrosis, mass extension to fourth ventricle for amen or magnum, and ADC values were documented for all patients. ADC was measured according to Taheri et al.'s method (12) (Figure 1). For every patient, the solid parts of tumors with enhancement were spotted on post-contrast T1W images and corresponding ADC maps. Then, the MRI scanner software automatically calculated ADC values by drawing the region of interest (ROI) on ADC maps.

Given that histopathologic examination is the gold standard for diagnosis of tumor type, all tumor histopathologic diagnoses were recorded for comparison with radiologic parameters.

This study conducted a statistical analysis to determine the sensitivity (true positive/[false negative + true positive]), specificity (true negative/[true negative + false positive], positive predictive value (PPV) (true positive/[false positive + true positive], and negative predictive value (NPV) (true negative/[true negative + false negative] of the CT and MRI features for the differentiation of medulloblastoma from

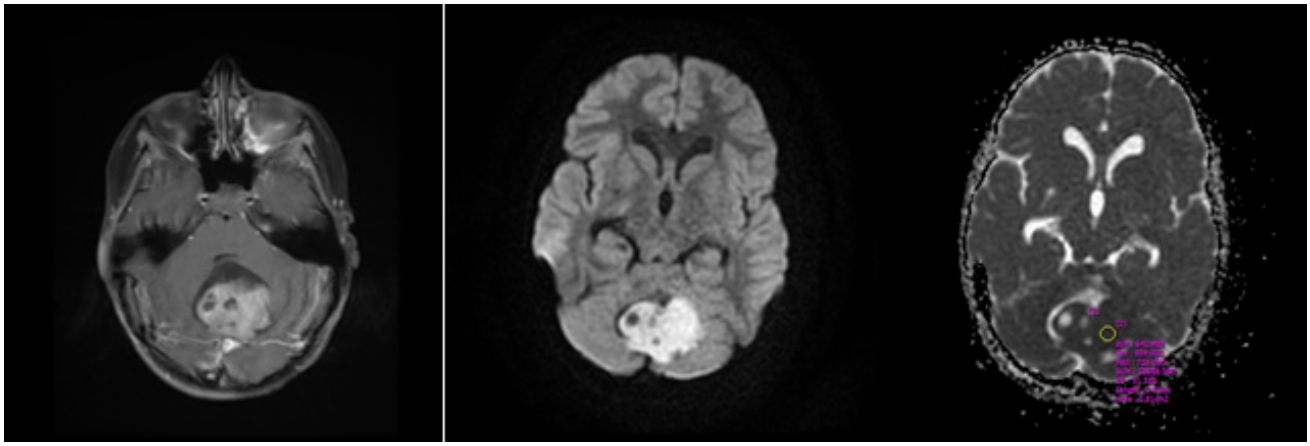

Figure 1. A: Contrast-enhanced axial T1 shows a midline enhancing lesion at the level of the fourth ventricle and vermis. B & C: DWI and ADC map shows the measurement of ADC value by placing the region of interest (ROI) in the non-cystic component of the mass

ependymoma, using histopathological diagnosis as the gold standard reference. The current study also used receiver-operating characteristic curve (ROC) analysis to determine the optimal cutoff values for MRI. The diagnostic performance of each imaging modality was evaluated using the area under the ROC curve (AUC). Statistical analysis was conducted using SPSS version 25.0 (IBM Corp., Armonk, NY, USA). A p-value of less than 0.05 was considered statistically significant.

Results

Forty-three patients with posterior fossa tumors were identified. Thirty-five patients compatible with the study criteria were included in the analysis, and eight patients were excluded (six cases of pilocytic astrocytoma, one case of hemangioblastoma, and one case of infiltrative glioma). Histopathologic diagnosis was medulloblastoma in 21 patients (60%) and ependymoma in 14 patients (40%).

Tumor morphology on MRI

Twelve cases of medulloblastoma (57.14%) and nine cases of ependymoma (64.28%) had heterogeneous tumors. Nine patients with medulloblastoma (42.85%) and five patients with ependymoma (35.71%) had homogeneous tumors. Statistical analysis showed no significant difference between medulloblastoma and ependymoma regarding tumor homogeneity on MRI (p=0.494) (Figures 2 & 3).

Four cases of medulloblastoma (19%) and six cases of ependymoma (42.9%) showed tumor extension to the fourth ventricle foramen or foramen magnum. The statistical difference between the two groups was not significant (p=0.127).

Cystic component in tumors was seen in 14 cases (66.7%) of medulloblastoma and seven cases of ependymoma (50%). Statistical analysis showed no significant difference between the two tumor types (p=0.324).

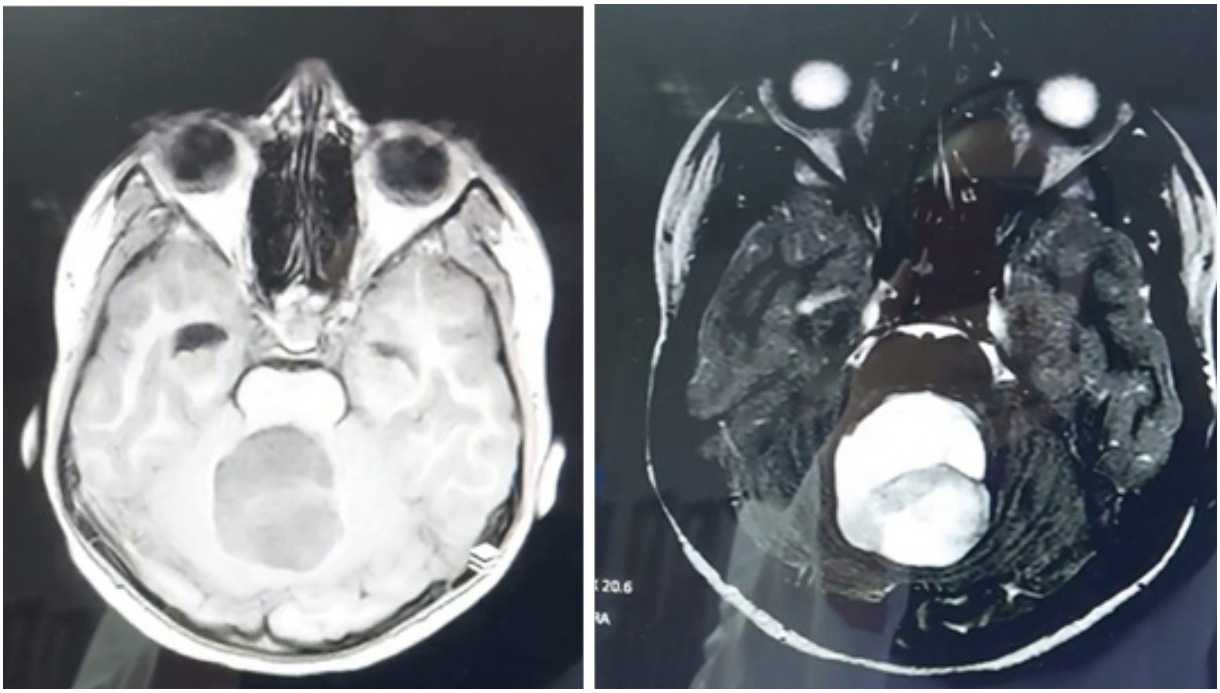

Figure 2. T1-weighted (left) and T2-weighted (right) images of ependymoma

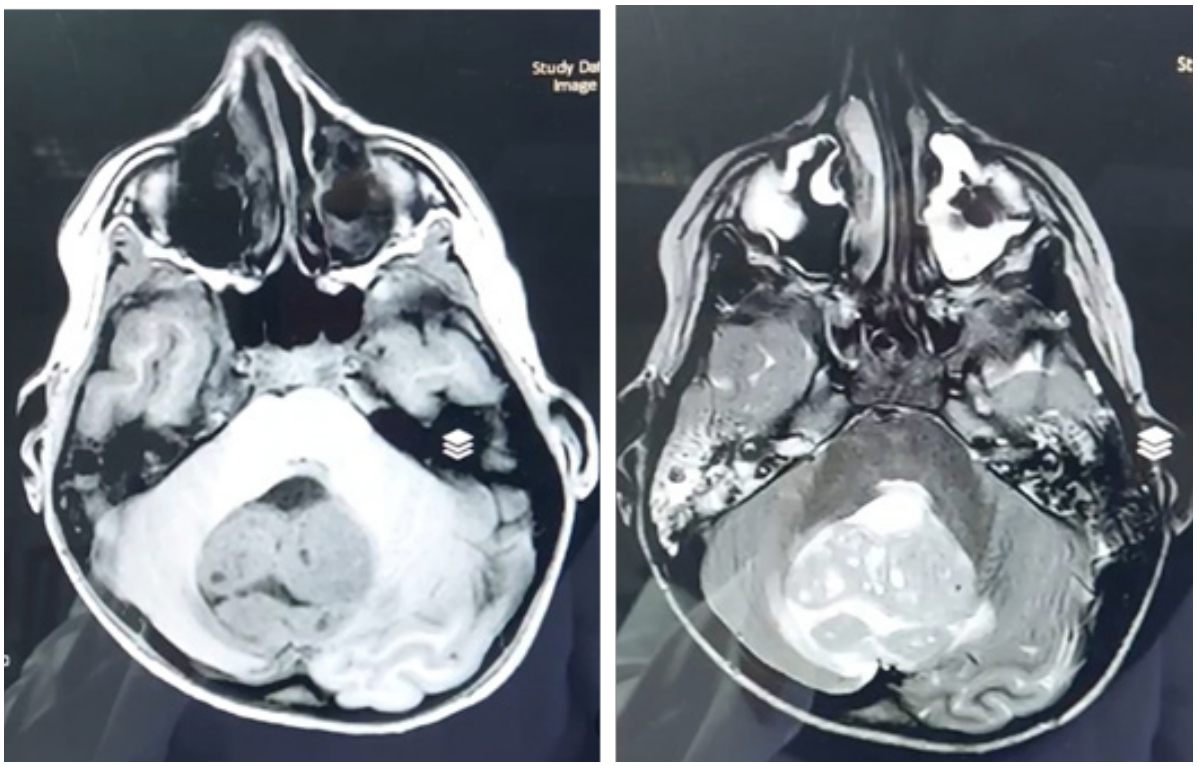

Figure 3. T1-weighted (left) and T2-weighted (right) images of Medulloblastoma

Signal Intensity on MRI

T1W images showed a hypointense signal in seven patients with medulloblastoma (38.09%) and eight patients with ependymoma (57.14%). Isointense signal was also seen in six patients (28.57%) with medulloblastoma and three patients (21.4%) with ependymoma (p=0.014). T2W images also demonstrated hyperintense signals in seven cases of medulloblastoma (33.3%) and nine ependymoma cases (64.28%). The isointense signal was also detected in three cases of ependymoma (21.4%), while ten cases (47.61%) of medulloblastoma exhibited an isointense signal (p=0.008).

Density of tumors on CT scan

Evaluation of tumor density compared to the adjacent brain tissue revealed hyperdense, isodense, and hypodense tumors in 14 (66.6%), three (14.28%), and two (9.52%) cases of medulloblastoma, respectively. Two cases of ependymoma (14.28%) were hyperdense, five cases (35.71%) were isodense, and six cases (42.85%) were hypodense (p=0.031).

Apparent diffusion coefficient (ADC) values

The mean ADC values in medulloblastoma cases were 0.67±0.19 (range= 0.50-1.25), while 1.22±0.29 (range=0.67-1.72) in ependymoma cases. The statistical analysis showed a significant difference between the two groups (p=0.000).

ROC analysis was performed to identify the most suitable ADC cut-off for differentiating medulloblastoma from ependymoma. The area under the curve (AUC) for this analysis was 0.936, indicating excellent efficacy. The ADC cut-off point of 0.9825 is associated with 90% sensitivity and 92.9% specificity for discriminating ependymoma from medulloblastoma (Figure 3). The diagnostic accuracy of the studied parameters is presented in Table 1.

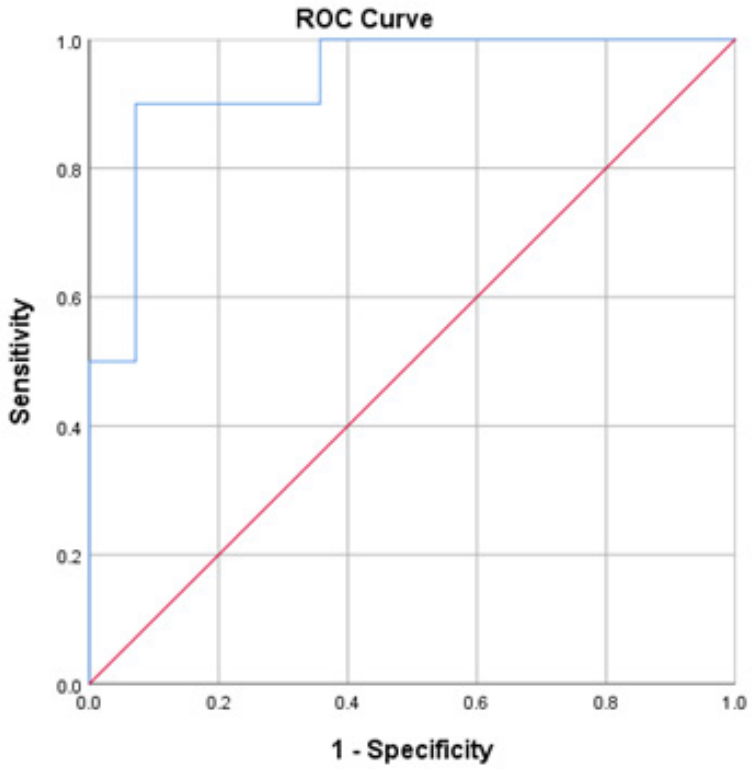

Figure 4. ROC curve for analysis of ADC values in differentiation of ependymoma from medulloblastoma

Table 1. Diagnostic accuracy of MRI and CT scan features for discrimination of medulloblastoma and ependymoma

Parameter	Sensitivity	Specificity	Positive predictive value (PPV) [95%CI]	Negative predictive value (NPV) [95%CI]
Heterogeneous morphology*	66.67%	45%	1.21 [0.69-2.13]	0.74 [0.29-1.89]
Tumor extension*	42.86%	80.95%	2.25 [0.77-6.55]	0.71 [0.43-1.16]
Cystic component*	50%	33.33%	0.75 [0.41-1.37]	1.50 [0.67-3.34]
Hemorrhagic component*	14.29%	95.24%	3 [0.30-30.02]	0.90 [0.71-1.14]
Hyperdensity on CT†	71.43%	83.33%	4.29 [0.67-27.24]	0.34 [0.10-1.17]
ADC value‡	90%	92.9%	2.44 [1.39-4.29]	0.12 [0.02-0.79]

*in favor of ependymoma
†in favor of medulloblastoma
‡≥0.9825 in favor of ependymoma

Discussion

Differentiating medulloblastoma from ependymoma is essential for planning suitable treatment strategies and improving patient outcomes. Although histopathological examination is the gold standard for definite diagnosis, imaging modalities play essential roles in the preoperative evaluation and provide clues for the diagnosis more conveniently and in less time than histopathological study.

This study aimed to compare the diagnostic accuracy of MRI and CT scan features in differentiating medulloblastoma from ependymoma. The results showed no significant difference between the two tumor types in terms of tumor morphology on MRI (heterogeneous tumor, cystic component, extension, or hemorrhage) or tumor density on CT scan. However, ADC values were significantly higher in ependymoma compared to medulloblastoma.

The higher ADC values in ependymoma compared to medulloblastoma observed in this study are consistent with previous studies. ADC values reflect the diffusion of water molecules within tissues and are influenced by several factors, including cellularity, extracellular matrix, and tissue microstructure. Ependymomas are typically less cellular and have a more open extracellular matrix than medulloblastomas, which may explain the higher ADC values observed in ependymoma (11-13).Taheri et al. have reported that mean ADC values for ependymoma have been significantly higher than medulloblastoma in the pediatric population (1.2±0.06 vs 0.87±0.02×$10^{-3}$$mm^2$/s, p = 0.041), indicating excellent efficacy it as a reliable method for differentiation of these malignancies (12). A recent meta-analysis by Dury et al. has revealed mean ADC values of 0.76±0.16 mm^2/s for medulloblastoma and 1.10±0.10 mm^2/s for ependymoma, which are significantly different. A cut-off value of 0.96 mm^2/s was also chosen for discrimination between medulloblastoma and ependymoma, with the highest sensitivity and specificity, which is quite similar to the ADC cut-off obtained in this study (14). Mohamed et al. also reported that ADC values range was 1 to 1.3 × 10^{-3} mm^2/s in the medulloblastoma group and 0.5 to 0.9× 10^{-3} mm^2/s in the ependymoma group with significant difference without any overlap (15). Consistent with the present findings, Rumboldt et al. indicated that ependymomas exhibited significantly higher ADC values compared to the medulloblastomas ($p<0.001$) (16). Another study by Mahmoud Esa et al. stated that ADC values were significantly higher in ependymomas than in medulloblastomas (1.04±0.21 vs 0.71±0.21×10^{-3} mm^2/s, $p<0.001$) (17). Novak et al. also revealed that an ADC cut-off value of 0.984× 10^{-3} mm^2/s was associated with 80.8% sensitivity and 80% specificity for differentiation of ependymoma from medulloblastoma in the pediatric population, which is quite similar to the current findings (18). These findings emphasize that ADC values are highly efficient in classifying posterior fossa tumors and discrimination between ependymoma and medulloblastoma.

Heterogeneous tumor morphology has been reported to be indicative of ependymoma over medulloblastoma tumors. However, this heterogeneous pattern overlaps with the diagnosis of medulloblastoma (9, 10). The obtained findings also showed that heterogeneous morphology has a sensitivity of 66% and specificity of 45% for diagnosing ependymoma, which is not a favorable diagnostic accuracy for this parameter.

Medulloblastomas are known to be hypercellular tumors with calcification. These features are believed to contribute to the hyperdensity of

medulloblastoma tumors on CT images. Few studies have been conducted on the discriminative role of CT hyperdensity in distinguishing medulloblastoma from ependymoma. Hyperdense tumors are reported to favor medulloblastoma over ependymoma (19-21). This study also confirmed this finding.

The main drawback of this study was its low sample size, which limited its statistical power. Future studies with more patients in future studies can provide more insight on this topic.

In Conclusion

In conclusion, the present study showed no significant difference between medulloblastoma and ependymoma regarding tumor morphology on MRI, but ADC values were significantly higher in ependymoma compared to medulloblastoma, suggesting the potential utility of DWI in differentiating these tumors. Further studies are needed to confirm the utility of DWI and other advanced MRI techniques in differentiating medulloblastoma from ependymoma.

Acknowledgment

The authors acknowledge Isfahan university of medical sciences، research department.
IR.MUI.MED.REC.1401.068

Authors' Contribution

Sam Mirfendereski evaluated the images, interpreted the findings, finalized the text, and supervised the project. Neda Mansouri collected the patients' information, analyzed the data, and prepared the manuscript draft.

Conflicts of Interest

Both authors declared no conflict of interest.

References

1. Baldwin RT, Preston-Martin S. Epidemiology of brain tumors in childhood-a review. Toxicol Appl Pharmacol 2004; 1992: 118–131.
2. Pollack IF. Brain tumors in children. N Engl J Med 1994; 331: 1500–1507.
3. Poretti A, Meoded A, Huisman TA. Neuroimaging of pediatric posterior fossa tumors including review of the literature. J Magn Reson Imaging. 2012 Jan;35(1):32-47. doi: 10.1002/jmri.22722. Epub 2011 Oct 11. PMID: 21989968.
4. Dhall G. Medulloblastoma. J Child Neurol 2009; 24: 1418–1430.
5. Davis FG, McCarthy BJ. Epidemiology of brain tumors. Curr Opin Neurol 2000; 13: 635–640.
6. Villano JL, Parker CK, Dolecek TA. Descriptive epidemiology of ependymal tumours in the United States. Br J Cancer. 2013 Jun 11;108(11):2367-71. doi: 10.1038/bjc.2013.221. Epub 2013 May 9. PMID: 23660944; PMCID: PMC3681017.
7. Dong J, Li L, Liang S, Zhao S, Zhang B, Meng Y, Zhang Y, Li S. Differentiation Between Ependymoma and Medulloblastoma in Children with Radiomics Approach. Acad Radiol. 2021 Mar;28(3):318-327. doi: 10.1016/j.acra.2020.02.012. Epub 2020 Mar 26. PMID: 32222329.
8. Albright AL. Pediatric brain tumors. CA 1993; 43:272–288.
9. Kobayashi K, Ando K, Kato F, Kanemura T, Imagama S, Sato K, et al. MRI characteristics of spinal ependymoma in WHO grade II: a review of 59 cases. Spine. 2018;43(9):E525-E30.
10. Kotani T, Okawa A, Akazawa T, Sakuma T. Mobile ependymoma diagnosed with cine MRI. Case Reports. 2014;2014:bcr2013202984

11. Xianwang L, Lei H, Hong L, Juan D, Shenglin L, Caiqiang X, et al. Apparent Diffusion Coefficient to Evaluate Adult Intracranial Ependymomas: Relationship to Ki-67 Proliferation Index. Journal of Neuroimaging. 2021;31(1):132-6.
12. Taheri H, Tavakoli MB. Measurement of Apparent Diffusion Coefficient (ADC) Values of Ependymoma and Medulloblastoma Tumors: a Patient-based Study. J Biomed Phys Eng. 2021 Feb 1;11(1):39-46. doi: 10.31661/jbpe.v0i0.889. PMID: 33564638; PMCID: PMC7859369.
13. Wang, T., Wu, X., Cui, Y. et al. Role of apparent diffusion coefficients with diffusion-weighted magnetic resonance imaging in differentiating between benign and malignant bone tumors. World J Surg Onc 12, 365 (2014). https://doi.org/10.1186/1477-7819-12-365
14. Dury RJ, Lourdusamy A, Macarthur DC, Peet AC, Auer DP, Grundy RG, Dineen RA. Meta-Analysis of Apparent Diffusion Coefficient in Pediatric Medulloblastoma, Ependymoma, and Pilocytic Astrocytoma. J Magn Reson Imaging. 2022 Jul;56(1):147-157. doi:10.1002/jmri.28007. Epub 2021 Nov 29. PMID: 34842328.
15. Mohamed, F. F., Azeem Ismail, A. A., Hasan, D. I., & Essa, W. E. (2013). The role of apparent diffusion coefficient (ADC) value in the differentiation between the most common pediatric posterior fossa tumors. The Egyptian Journal of Radiology and Nuclear Medicine, 44(2), 349-355. doi:https://doi.org/10.1016/j.ejrnm.2012.12.011
16. Rumboldt Z, Camacho D L, Lake D, Welsh C T, Castillo M. Apparent diffusion coefficients for differentiation of cerebellar tumors in children. AJNR Am J Neuroradiol. 2006;27:1362–9.
17. Esa, M.M.M., Mashaly, E.M., El-Sawaf, Y.F. et al. Diagnostic accuracy of apparent diffusion coefficient ratio in distinguishing common pediatric CNS posterior fossa tumors. Egypt J Radiol Nucl Med 51, 76 (2020). https://doi.org/10.1186/s43055-020-00194-2
18. Novak, J., Zarinabad, N., Rose, H. et al. Classification of paediatric brain tumours by diffusion weighted imaging and machine learning. Sci Rep 11, 2987 (2021).
19. Duc NM. The effect of semi-quantitative T1-perfusion parameters for the differentiation between pediatric medulloblastoma and ependymoma. Egyptian Journal of Radiology and Nuclear Medicine. 2020;51(1):1-6.
20. Duc NM, Huy HQ, Nadarajan C, Keserci B. The role of predictive model based on quantitative basic magnetic resonance imaging in differentiating medulloblastoma from ependymoma. Anticancer research. 2020;40(5):2975-80.
21. Eran A, Ozturk A, Aygun N, Izbudak I. Medulloblastoma: atypical CT and MRI findings in children. Pediatric radiology. 2010;40(7):1254-62.